

Net Charge Fluctuations in Au + Au Interactions
at $\sqrt{s_{NN}} = 130$ GeV

K. Adcox,⁴⁰ S. S. Adler,³ N. N. Ajitanand,²⁷ Y. Akiba,¹⁴ J. Alexander,²⁷ L. Aphecetche,³⁴ Y. Arai,¹⁴ S. H. Aronson,³ R. Averbeck,²⁸ T. C. Awes,²⁹ K. N. Barish,⁵ P. D. Barnes,¹⁹ J. Barrette,²¹ B. Bassalleck,²⁵ S. Bathe,²² V. Baublis,³⁰ A. Bazilevsky,^{12,32} S. Belikov,^{12,13} F. G. Bellaiche,²⁹ S. T. Belyaev,¹⁶ M. J. Bennett,¹⁹ Y. Berdnikov,³⁵ S. Botelho,³³ M. L. Brooks,¹⁹ D. S. Brown,²⁶ N. Bruner,²⁵ D. Bucher,²² H. Buesching,²² V. Bumazhnov,¹² G. Bunce,^{3,32} J. Burward-Hoy,²⁸ S. Butsyk,^{28,30} T. A. Carey,¹⁹ P. Chand,² J. Chang,⁵ W. C. Chang,¹ L. L. Chavez,²⁵ S. Chernichenko,¹² C. Y. Chi,⁸ J. Chiba,¹⁴ M. Chiu,⁸ R. K. Choudhury,² T. Christ,²⁸ T. Chujo,^{3,39} M. S. Chung,^{15,19} P. Chung,²⁷ V. Cianciolo,²⁹ B. A. Cole,⁸ D. G. D'Enterria,³⁴ G. David,³ H. Delagrangé,³⁴ A. Denisov,¹² A. Deshpande,³² E. J. Desmond,³ O. Dietzsch,³³ B. V. Dinesh,² A. Drees,²⁸ A. Durum,¹² D. Dutta,² K. Ebisu,²⁴ Y. V. Efremenko,²⁹ K. El Chenawi,⁴⁰ H. En'yo,^{17,31} S. Esumi,³⁹ L. Ewell,³ T. Ferdousi,⁵ D. E. Fields,²⁵ S. L. Fokin,¹⁶ Z. Fraenkel,⁴² A. Franz,³ A. D. Frawley,⁹ S.-Y. Fung,⁵ S. Garpman,^{20,*} T. K. Ghosh,⁴⁰ A. Glenn,³⁶ A. L. Godoi,³³ Y. Goto,³² S. V. Greene,⁴⁰ M. Grosse Perdekamp,³² S. K. Gupta,² W. Guryn,³ H.-Å. Gustafsson,²⁰ J. S. Haggerty,³ H. Hamagaki,⁷ A. G. Hansen,¹⁹ H. Hara,²⁴ E. P. Hartouni,¹⁸ R. Hayano,³⁸ N. Hayashi,³¹ X. He,¹⁰ T. K. Hemmick,²⁸ J. M. Heuser,²⁸ M. Hibino,⁴¹ J. C. Hill,¹³ D. S. Ho,⁴³ K. Homma,¹¹ B. Hong,¹⁵ A. Hoover,²⁶ T. Ichihara,^{31,32} K. Imai,^{17,31} M. S. Ippolitov,¹⁶ M. Ishihara,^{31,32} B. V. Jacak,^{28,32} W. Y. Jang,¹⁵ J. Jia,²⁸ B. M. Johnson,³ S. C. Johnson,^{18,28} K. S. Joo,²³ S. Kametani,⁴¹ J. H. Kang,⁴³ M. Kann,³⁰ S. S. Kapoor,² S. Kelly,⁸ B. Khachaturov,⁴² A. Khanzadeev,³⁰ J. Kikuchi,⁴¹ D. J. Kim,⁴³ H. J. Kim,⁴³ S. Y. Kim,⁴³ Y. G. Kim,⁴³ W. W. Kinnison,¹⁹ E. Kistenev,³ A. Kiyomichi,³⁹ C. Klein-Boesing,²² S. Klinksiek,²⁵ L. Kochenda,³⁰ V. Kochetkov,¹² D. Koehler,²⁵ T. Kohama,¹¹ D. Kotchetkov,⁵ A. Kozlov,⁴² P. J. Kroon,³ K. Kurita,^{31,32} M. J. Kweon,¹⁵ Y. Kwon,⁴³ G. S. Kyle,²⁶ R. Lacey,²⁷ J. G. Lajoie,¹³ J. Lauret,²⁷ A. Lebedev,^{13,16} D. M. Lee,¹⁹ M. J. Leitch,¹⁹ X. H. Li,⁵ Z. Li,^{6,31} D. J. Lim,⁴³ M. X. Liu,¹⁹ X. Liu,⁶ Z. Liu,⁶ C. F. Maguire,⁴⁰ J. Mahon,³ Y. I. Makdisi,³ V. I. Manko,¹⁶ Y. Mao,^{6,31} S. K. Mark,²¹ S. Markacs,⁸ G. Martinez,³⁴ M. D. Marx,²⁸ A. Masaike,¹⁷ F. Matathias,²⁸ T. Matsumoto,^{7,41} P. L. McGaughey,¹⁹ E. Melnikov,¹² M. Merschmeyer,²² F. Messer,²⁸ M. Messer,³ Y. Miake,³⁹ T. E. Miller,⁴⁰ A. Milov,⁴² S. Mioduszewski,^{3,36} R. E. Mischke,¹⁹ G. C. Mishra,¹⁰ J. T. Mitchell,³ A. K. Mohanty,² D. P. Morrison,³ J. M. Moss,¹⁹ F. Mühlbacher,²⁸ M. Muniruzzaman,⁵ J. Murata,³¹ S. Nagamiya,¹⁴ Y. Nagasaka,²⁴ J. L. Nagle,⁸ Y. Nakada,¹⁷ B. K. Nandi,⁵ J. Newby,³⁶ L. Nikkinen,²¹ P. Nilsson,²⁰ S. Nishimura,⁷ A. S. Nyanin,¹⁶ J. Nystrand,²⁰ E. O'Brien,³ C. A. Ogilvie,¹³ H. Ohnishi,^{3,11} I. D. Ojha,^{4,40} M. Ono,³⁹ V. Onuchin,¹² A. Oskarsson,²⁰ L. Österman,²⁰ I. Otterlund,²⁰ K. Oyama,^{7,38} L. Paffrath,^{3,*} A. P. T. Palounek,¹⁹ V. S. Pantuev,²⁸ V. Papavassiliou,²⁶ S. F. Pate,²⁶ T. Peitzmann,²² A. N. Petridis,¹³ C. Pinkenburg,^{3,27} R. P. Pisani,³ P. Pitukhin,¹² F. Plasil,²⁹ M. Pollack,^{28,36} K. Pope,³⁶ M. L. Purschke,³ I. Ravinovich,⁴² K. F. Read,^{29,36} K. Reygers,²² V. Riabov,^{30,35} Y. Riabov,³⁰ M. Rosati,¹³ A. A. Rose,⁴⁰ S. S. Ryu,⁴³ N. Saito,^{31,32} A. Sakaguchi,¹¹ T. Sakaguchi,^{7,41} H. Sako,³⁹ T. Sakuma,^{31,37} V. Samsonov,³⁰ T. C. Sangster,¹⁸ R. Santo,²² H. D. Sato,^{17,31} S. Sato,³⁹ S. Sawada,¹⁴ B. R. Schlei,¹⁹ Y. Schutz,³⁴ V. Semenov,¹² R. Seto,⁵ T. K. Shea,³ I. Shein,¹² T. -A. Shibata,^{31,37} K. Shigaki,¹⁴ T. Shiina,¹⁹ Y. H. Shin,⁴³ I. G. Sibiriyak,¹⁶ D. Silvermyr,²⁰ K. S. Sim,¹⁵ J. Simon-Gillo,¹⁹ C. P. Singh,⁴ V. Singh,⁴ M. Sivertz,³ A. Soldatov,¹² R. A. Soltz,¹⁸ S. Sorensen,^{29,36} P. W. Stankus,²⁹ N. Starinsky,²¹ P. Steinberg,⁸ E. Stenlund,²⁰ A. Ster,⁴⁴ S. P. Stoll,³ M. Sugioka,^{31,37} T. Sugitate,¹¹ J. P. Sullivan,¹⁹ Y. Sumi,¹¹ Z. Sun,⁶ M. Suzuki,³⁹ E. M. Takagui,³³ A. Taketani,³¹ M. Tamai,⁴¹ K. H. Tanaka,¹⁴ Y. Tanaka,²⁴ E. Taniguchi,^{31,37} M. J. Tannenbaum,³ J. Thomas,²⁸ J. H. Thomas,¹⁸ T. L. Thomas,²⁵ W. Tian,^{6,36} J. Tojo,^{17,31} H. Torii,^{17,31} R. S. Towell,¹⁹ I. Tserruya,⁴² H. Tsuruoka,³⁹ A. A. Tsvetkov,¹⁶ S. K. Tuli,⁴ H. Tydesjö,²⁰ N. Tyurin,¹² T. Ushiroda,²⁴ H. W. van Hecke,¹⁹ C. Velissaris,²⁶ J. Velkovska,²⁸ M. Velkovsky,²⁸ A. A. Vinogradov,¹⁶ M. A. Volkov,¹⁶ A. Vorobyov,³⁰ E. Vznuzdaev,³⁰ H. Wang,⁵ Y. Watanabe,^{31,32} S. N. White,³ C. Witzig,³ F. K. Wohn,¹³ C. L. Woody,³ W. Xie,^{5,42} K. Yagi,³⁹ S. Yokkaichi,³¹ G. R. Young,²⁹ I. E. Yushmanov,¹⁶ W. A. Zajc,⁸ Z. Zhang,²⁸ and S. Zhou⁶

(PHENIX Collaboration)

¹*Institute of Physics, Academia Sinica, Taipei 11529, Taiwan*

²*Bhabha Atomic Research Centre, Bombay 400 085, India*

³*Brookhaven National Laboratory, Upton, NY 11973-5000, USA*

⁴*Department of Physics, Banaras Hindu University, Varanasi 221005, India*

⁵*University of California - Riverside, Riverside, CA 92521, USA*

⁶*China Institute of Atomic Energy (CIAE), Beijing, People's Republic of China*

⁷*Center for Nuclear Study, Graduate School of Science, University of Tokyo, 7-3-1 Hongo, Bunkyo, Tokyo 113-0033, Japan*

⁸*Columbia University, New York, NY 10027 and Nevis Laboratories, Irvington, NY 10533, USA*

⁹*Florida State University, Tallahassee, FL 32306, USA*

¹⁰*Georgia State University, Atlanta, GA 30303, USA*

¹¹*Hiroshima University, Kagamiyama, Higashi-Hiroshima 739-8526, Japan*

- ¹²*Institute for High Energy Physics (IHEP), Protvino, Russia*
¹³*Iowa State University, Ames, IA 50011, USA*
¹⁴*KEK, High Energy Accelerator Research Organization, Tsukuba-shi, Ibaraki-ken 305-0801, Japan*
¹⁵*Korea University, Seoul, 136-701, Korea*
¹⁶*Russian Research Center "Kurchatov Institute", Moscow, Russia*
¹⁷*Kyoto University, Kyoto 606, Japan*
¹⁸*Lawrence Livermore National Laboratory, Livermore, CA 94550, USA*
¹⁹*Los Alamos National Laboratory, Los Alamos, NM 87545, USA*
²⁰*Department of Physics, Lund University, Box 118, SE-221 00 Lund, Sweden*
²¹*McGill University, Montreal, Quebec H3A 2T8, Canada*
²²*Institut für Kernphysik, University of Münster, D-48149 Münster, Germany*
²³*Myongji University, Yongin, Kyonggido 449-728, Korea*
²⁴*Nagasaki Institute of Applied Science, Nagasaki-shi, Nagasaki 851-0193, Japan*
²⁵*University of New Mexico, Albuquerque, NM 87131, USA*
²⁶*New Mexico State University, Las Cruces, NM 88003, USA*
²⁷*Chemistry Department, State University of New York - Stony Brook, Stony Brook, NY 11794, USA*
²⁸*Department of Physics and Astronomy, State University of New York - Stony Brook, Stony Brook, NY 11794, USA*
²⁹*Oak Ridge National Laboratory, Oak Ridge, TN 37831, USA*
³⁰*PNPI, Petersburg Nuclear Physics Institute, Gatchina, Russia*
³¹*RIKEN (The Institute of Physical and Chemical Research), Wako, Saitama 351-0198, JAPAN*
³²*RIKEN BNL Research Center, Brookhaven National Laboratory, Upton, NY 11973-5000, USA*
³³*Universidade de São Paulo, Instituto de Física, Caixa Postal 66318, São Paulo CEP05315-970, Brazil*
³⁴*SUBATECH (Ecole des Mines de Nantes, IN2P3/CNRS, Universite de Nantes) BP 20722 - 44307, Nantes-cedex 3, France*
³⁵*St. Petersburg State Technical University, St. Petersburg, Russia*
³⁶*University of Tennessee, Knoxville, TN 37996, USA*
³⁷*Department of Physics, Tokyo Institute of Technology, Tokyo, 152-8551, Japan*
³⁸*University of Tokyo, Tokyo, Japan*
³⁹*Institute of Physics, University of Tsukuba, Tsukuba, Ibaraki 305, Japan*
⁴⁰*Vanderbilt University, Nashville, TN 37235, USA*
⁴¹*Waseda University, Advanced Research Institute for Science and Engineering, 17 Kikui-cho, Shinjuku-ku, Tokyo 162-0044, Japan*
⁴²*Weizmann Institute, Rehovot 76100, Israel*
⁴³*Yonsei University, IPAP, Seoul 120-749, Korea*
⁴⁴*KFKI Research Institute for Particle and Nuclear Physics (RMKI), Budapest, Hungary[†]*
(October 31, 2018)

Data from Au + Au interactions at $\sqrt{s_{NN}} = 130$ GeV, obtained with the PHENIX detector at RHIC, are used to investigate local net charge fluctuations among particles produced near mid-rapidity. According to recent suggestions, such fluctuations may carry information from the Quark Gluon Plasma. This analysis shows that the fluctuations are dominated by a stochastic distribution of particles, but are also sensitive to other effects, like global charge conservation and resonance decays.

PACS numbers: 25.75.Dw

The PHENIX detector [1] at the Relativistic Heavy-Ion Collider (RHIC) is a versatile detector designed to study the properties of nuclear matter at extreme temperatures and energy densities, obtained in central heavy-ion collisions at ultra-relativistic energies. A central goal of these studies is to collect evidence for the existence of the Quark-Gluon Plasma (QGP) characterized by deconfined quarks and gluons.

There are several proposed ways to experimentally verify the existence of a QGP [2]. A general problem is that many of these signals also can be produced in a hadronic scenario, albeit special conditions of highly compressed matter have to prevail. Furthermore, it is not straightforward to determine how the various plasma signals are

distorted when the deconfined matter transforms back to hadronic matter. Recent theoretical investigations [3–5] predict a drastic decrease of the event-by-event fluctuations of the net charge in local phase-space regions as a signature of the plasma state. These fluctuations are not related to the transition itself, but rather with the charge distribution in the primordial plasma state. The basic idea is that each of the charge carriers in the plasma carries less charge than the charge carriers in ordinary hadronic matter. The charge will thus be more evenly distributed in a plasma. The main concern of the theoretical discussions is how and why the original distribution survives the transition back to ordinary matter [6,7]. Predictions, for a rapidity coverage $\Delta y \geq 1$, range up to

an 80% reduction in the magnitude of the fluctuations, as measured by the variance of the net charge.

Decays of hadronic resonances influence the net charge fluctuations, whether or not deconfinement is reached. In the absence of a QGP, deviations from statistical behaviour can be used to determine the abundance of e.g. ρ and ω mesons [8]. In a hadron gas resonances are expected to decrease the fluctuations by about 25%. Globally, fluctuations will be further reduced, since charge is a conserved quantity. Deviations from a statistical behaviour in the net charge are also of relevance when the phase transition is treated as a semiclassical decay of a Polyakov loop condensate [9]. Although multiplicity fluctuations have been studied extensively in both hadronic and nuclear processes [10], net charge fluctuations have not been addressed experimentally.

In this Letter we report results from an analysis of net charge fluctuations for particles produced in Au+Au interactions at $\sqrt{s_{NN}} = 130$ GeV. The fluctuations are studied in the variables $R = n_+/n_-$, the ratio between positive and negative particles, and $Q = n_+ - n_-$, the net charge [3]. The advantages and disadvantages of these variables will also be discussed.

Information from one of the PHENIX central tracking arms (west) is used in this analysis, where events are required to have a well-defined vertex close to the center of the apparatus ($|Z| < 17$ cm), as defined by the two beam-beam counters (BBC). These are Cherenkov-counters surrounding the beam, placed on both sides 1.44 m from the interaction region, covering the pseudorapidity region $3.0 < |\eta| < 3.9$. Together with the information from the two zero-degree calorimeters (ZDC), placed further away (18 m), the BBC information is used for off-line centrality selection [11]. A total of about 5×10^5 minimum bias events has been analyzed. The PHENIX west arm spectrometer has an acceptance of 0.7 units of pseudorapidity ($-0.35 < \eta < 0.35$) and $\pi/2$ radians in azimuth φ . Charged-particle trajectories are recorded in a multiwire focusing drift chamber (DC) [12]. The combination of reconstructed DC tracks [13] with matching hits in the innermost pad-chamber plane (PC1) defines the sign of the charge of the particle and also provides a high resolution measurement of the transverse momentum p_T of tracks originating from the collision vertex. Tracks with a reconstructed p_T less than 0.2 GeV/c have been excluded from the analysis due to a low reconstruction efficiency and large contributions from background sources, as revealed by simulations.

The tracking efficiency and the charge assignment have been studied using GEANT [14] simulations. Of particular importance in this context is a realistic description of the drift chamber response. The drift distances have been calculated based on a geometric model of the individual drift cells. Additional parameters describing the response of the chamber, i.e. single-wire efficiency, pulse width, single-hit resolution, and space drift-time relation,

have been extracted from measured data, parameterized, and applied empirically in the simulation.

RQMD [15] simulations are used to study the detection efficiency, and the fraction of reconstructed particles that preserve their charge, as well as to evaluate the results of the analysis. The charge fluctuations in RQMD are consistent with calculations based on other hadronic models like UrQMD and HIJING [3]. The overall efficiency for detecting a charged particle within the acceptance is found to be around 80% for both positive and negative particles. Depending on p_T , between 70% and 85% of the reconstructed tracks are in one-to-one correspondence with a primarily produced particle. The remaining tracks come from secondary interactions in the detector material and from decays, where the original charge information is lost.

In each event the numbers of positively charged particles n_+ , negatively charged particles n_- , and their sum n_{ch} are recorded. In a stochastic scenario, with a fixed number of charged particles within the acceptance, where each particle is assigned a random charge (+1 or -1 with the same probability), the variance of the net charge, Q , is

$$V(Q) \equiv \langle Q^2 \rangle - \langle Q \rangle^2 = n_{ch}. \quad (0.1)$$

The normalized variance in Q is

$$v(Q) \equiv \frac{V(Q)}{n_{ch}} = 1. \quad (0.2)$$

For the charge ratio, in the stochastic scenario, $V(R) \equiv \langle R^2 \rangle - \langle R \rangle^2$ will approach the value $4/n_{ch}$ as n_{ch} increases and $v(R) \equiv n_{ch} \cdot V(R)$ asymptotically approaches 4. A small asymmetry between positive and negative particles affects $v(R)$ drastically, whereas the effect on $v(Q)$ is negligible. If we write the probability p_+ , that a given particle has positive charge, in the form $p_+ = 1/2(1 + \varepsilon)$, and subsequently $p_- = 1/2(1 - \varepsilon)$, we find

$$v(Q) = 1 - \varepsilon^2, \quad (0.3)$$

while the asymptotic value of $v(R)$ is $4 + 16\varepsilon + O(\varepsilon^2)$. Detector or reconstruction inefficiencies do not influence those results in the stochastic scenario. To calculate $v(Q)$ as a function of multiplicity, Eq. 0.3 can be used and $v(R)$ can be calculated from

$$\langle R \rangle = \frac{1}{A} \sum_{i=1}^{n_{ch}-1} \frac{n_{ch}-i}{i} \binom{n_{ch}}{i} p_+^{n_{ch}-i} p_-^i, \quad (0.4)$$

and

$$\langle R^2 \rangle = \frac{1}{A} \sum_{i=1}^{n_{ch}-1} \left(\frac{n_{ch}-i}{i} \right)^2 \binom{n_{ch}}{i} p_+^{n_{ch}-i} p_-^i, \quad (0.5)$$

where $A = 1 - p_+^{n_{ch}} - p_-^{n_{ch}}$ is the new normalization due to discarding events with n_+ or n_- equal to zero. The

variance of R , even for a purely stochastic charge distribution, depends on multiplicity and on the fractions of positive and negative particles.

The data show a small excess of positive particles, growing proportionally with n_{ch} , in qualitative agreement with calculations using RQMD and GEANT. A part of this excess comes from the intrinsic isospin asymmetry and a part from secondary interactions in the detector and surrounding materials.

In Fig. 1a, $v(R)$ and $v(Q)$ are displayed as functions of n_{ch} . $v(Q)$ is multiplied by a factor of 4 to compensate for the asymptotical difference between $v(R)$ and $v(Q)$. Both $v(Q)$ and $v(R)$ are well described by the results obtained from the stochastic scenario, including the positive excess, as given by the curves.

Since $v(Q)$ is independent of n_{ch} one expects $v(Q)$ to be close to unity also in representations where other centrality measures are used. On the other hand, since $v(R)$ depends on multiplicity, it will have a complicated behaviour as a function of centrality, making it difficult to draw any further conclusions. We will thus focus on $v(Q)$ for the rest of this analysis.

In Fig. 1b, $v(Q)$ is displayed as a function of centrality based on the ZDC/BBC information. The full event sample, corresponding to 92% of the inelastic cross section [11], is divided into 20 centrality classes, where each class corresponds to 5% of the events. Class 20 represents the most central events. With the increased resolution on the y-axis in Fig. 1b, it is evident that $v(Q)$ is consistently below unity, and deviates from stochastic behaviour. The value is, however, far above the most optimistic QGP predictions $v(Q) \sim 0.2$ [3], although one should keep in mind that our coverage in rapidity is on the limit for these predictions and that we have only partial coverage in azimuth.

There may be other explanations for deviations from stochastic behaviour than the one offered by the quark-gluon plasma. These include global charge conservation and neutral resonances decaying into correlated pairs of one positive and one negative particle. Both of these effects will decrease the fluctuations, and the decrease will grow in proportion to the experimental acceptance. In a stochastic scenario, taking global charge conservation into account, the normalized variance $v(Q)$ becomes $(1-p)$, where p is the fraction of observed charged particles among all charged particles in the event. Eventually, if all charged particles are detected, $v(Q)$ will become 0.

Experimentally we can change the fraction p of particles within the acceptance by using different regions of the PHENIX west arm. In Fig. 2, $v(Q)$, for the 10 % most central events, is displayed as a function of $\Delta\varphi_d$, i.e. the chosen azimuthal interval of the spectrometer. For comparison, the results from RQMD processed through GEANT are shown. The data and the simulation show a similar trend. Note that the errors given are correlated, since the data in one bin are a subset of the data in the

next. The solid line corresponds to the $(1-p)$ dependence discussed above. The linear relationship between p and $\Delta\varphi_d$ is estimated from the phase-space distribution of particles in RQMD, including effects from reconstruction efficiency and background tracks. For larger angles, both data and the RQMD results lie consistently below the line, which indicates that effects from resonance decays are important.

Due to the influence of the magnetic field the positive and negative particles will have different azimuthal acceptance. The $\Delta\varphi_d$ study in Fig. 2 thus selects partly non-overlapping regions of phase space for positive and negative particles. A remedy for this is to use the reconstructed φ -angle for each particle φ_r , i.e. the azimuthal direction of the particle at the primary vertex, before it is deflected by the magnetic field. Figure 3a shows the acceptance in transverse momentum and φ_r for positive and negative particles. By choosing the azimuthal interval $\Delta\varphi_r$ symmetrically around the center of the acceptance, a better phase space overlap is achieved for small azimuthal intervals. In Fig. 3b, $v(Q)$, for the 10 % most central events, is displayed as a function of $\Delta\varphi_r$. The $(1-p)$ dependence, which is no longer linear, is given by the solid curve. Again data and the RQMD results show a similar trend, but the deviations from the curve are larger in this representation, indicating that an overlap in phase space is of importance. For large values of $\Delta\varphi$, the acceptance approaches the limits determined by the boundaries of the tracking arm, and the two representations are essentially the same.

The effects of the detector inefficiency and background tracks not assigned the correct charge have been investigated in a Monte Carlo simulation. It is assumed that the inefficiency independently removes positive and negative particles with the same probability, and that the background consists of uncorrelated positive and negative particles. The reconstruction efficiency and the amount of background have been determined from the RQMD and GEANT simulations discussed earlier. Both the inefficiency and the background contribution have the effect of diluting the signal and pushing the value of $v(Q)$ closer to 1. The dilution due to these effects can be treated as an experimental systematic error, estimated from the simulations, setting a lower limit on $v(Q)$. For the net charge fluctuations in the region $-0.35 < \eta < 0.35$, $p_T > 0.2$ GeV/c, $\Delta\varphi = \pi/2$,

$$v(Q) = 0.965 \pm 0.007(stat.) - 0.019(syst.) \quad (0.6)$$

is obtained for the 10 % most central events. A linear extrapolation of this value to full azimuthal coverage gives a value of $v(Q)$ in the range 0.78 - 0.86, in qualitative agreement with calculations from a hadronic gas. For comparison, it would be desirable to have a Monte Carlo model for the QGP which exhibits the predicted reduction in the charge fluctuations and which could be used

to study the sensitivity of the method for limited acceptance.

To summarize, we have shown that the data behave in an almost stochastic manner. There are also clear indications that effects from hadronic decays are seen; the data are in good agreement with RQMD calculations, which includes the effects of global charge conservations as well as neutral hadronic resonance decays. Furthermore, the data show no centrality dependence, which is in contradiction to the expectations from a Quark-Gluon Plasma scenario. We have clearly demonstrated that the fluctuations of the charge ratio $v(R)$ and of the net charge $v(Q)$ are well understood in a stochastic model. We, however, advise against the usage of the proposed R variable [3], since it unnecessarily complicates the evaluation of the fluctuations, and the intrinsic decrease of $v(R)$, as a function of centrality, can be mistaken as a 'plasma fingerprint'. The measured value of $v(Q) = 0.965$ is far from the value predicted for a plasma. Even extrapolating the linear trend seen in the data in Fig. 2 to full azimuthal coverage, renders values of the fluctuations, which are far above the proposed values. With the caveat of our limited acceptance in rapidity, these results clearly indicate either the absence of a plasma or that the proposed signal does not survive the transition back to hadronic matter.

We thank the staff of the Collider-Accelerator and Physics Departments at BNL for their vital contributions. We acknowledge support from the Department of Energy and NSF (U.S.A.), Monbu-sho and STA (Japan), RAS, RMAE, and RMS (Russia), BMBF, DAAD, and AvH (Germany), VR and KAW (Sweden), MIST and NSERC (Canada), CNPq and FAPESP (Brazil), IN2P3/CNRS (France), DAE and DST (India), KRF and CHEP (Korea), the U.S. CRDF for the FSU, and the US-Israel BSF.

* Deceased

† Not a participating Institution.

- [1] PHENIX Collaboration, D. P. Morrison, *et al.*, Nucl. Phys. **A638**, 565c (1998).
 [2] see e.g. J.-P. Blaizot, Nucl. Phys. **A661**, 3c (1999).
 [3] S. Jeon and V. Koch, Phys. Rev. Lett. **85**, 2076 (2000); M. Bleicher, S. Jeon and V. Koch, Phys. Rev. **C62**, 061902(R) (2000).
 [4] M. Asakawa, U. Heinz and B Müller, Phys. Rev. Lett. **85**, 2072 (2000).
 [5] H. Heiselberg and A. D. Jackson, Phys. Rev. **C63**, 064904 (2001).
 [6] E. V. Shuryak and M. A. Stephanov, Phys.Rev. **C63**, 064903 (2001).
 [7] K. Fialkowski and R. Wit, Europhys. Lett. **55** (2), 184 (2001).

- [8] S. Jeon and V. Koch, Phys. Rev. Lett. **83**, 5435 (1999).
 [9] A. Dumitru and R. D. Pisarski, Phys. Lett. **B504**, 282 (2001).
 [10] see e.g. E.A. De Wolf, I.M. Dremin and W. Kittel, Phys. Rep. **270**, 48 (1996).
 [11] PHENIX Collaboration, K. Adcox, *et al.*, Phys. Rev. Lett. **86**, 3500 (2001).
 [12] V. G. Riabov, Nucl. Instr. and Methods **A 419**, 363 (1998).
 [13] J. T. Mitchell *et al.*, nucl-ex/0201013, accepted for publication in Nuclear Instr. and Methods A.
 [14] GEANT 3.2.1, CERN program library.
 [15] H. Sorge, Phys. Rev. **C 52** 3291 (1995).

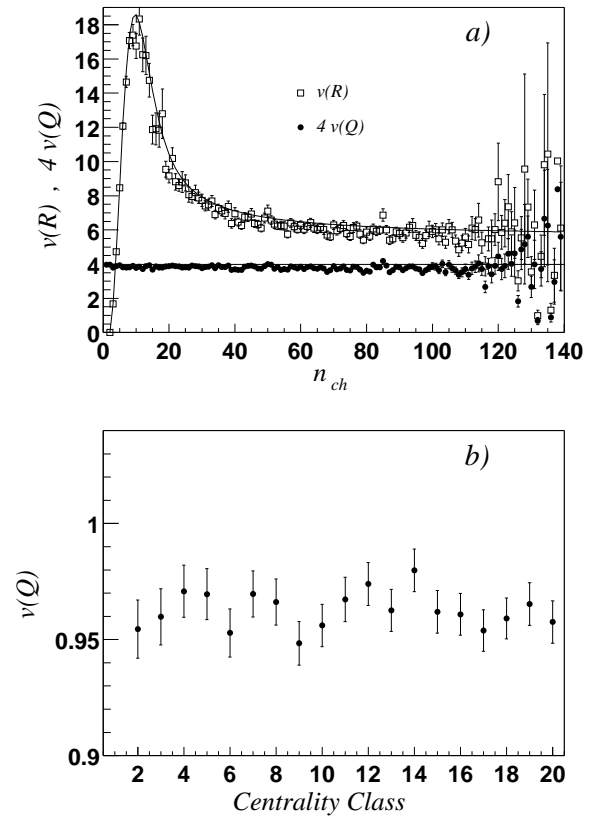


FIG. 1. a) The normalized variances $v(Q)$ and $v(R)$ as functions of n_{ch} , together with curves for stochastic behaviour. b) The normalized variance $v(Q)$ for different centrality classes, as described in the text.

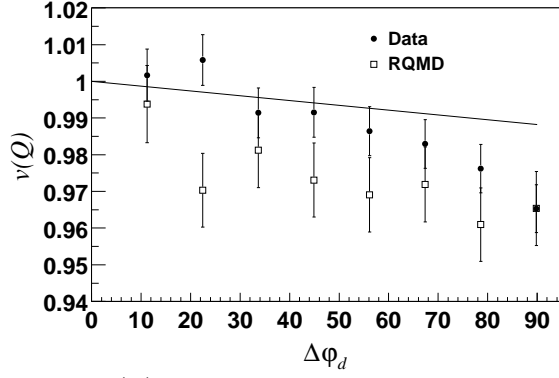


FIG. 2. $v(Q)$, for central events, as a function of the azimuthal coverage of the detector for data and events simulated with the RQMD model. The solid line shows the expected reduction in $v(Q)$ in the stochastic scenario when global charge conservation is taken into account. (Angles in degrees.)

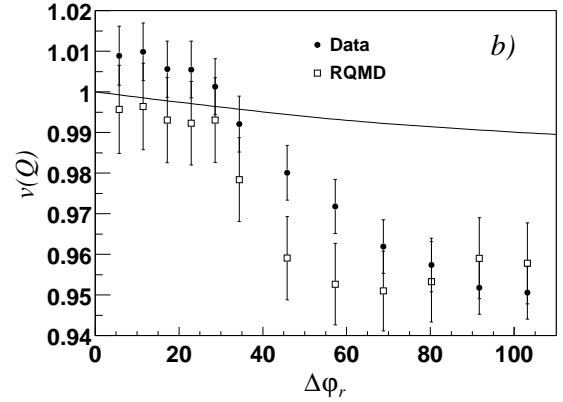
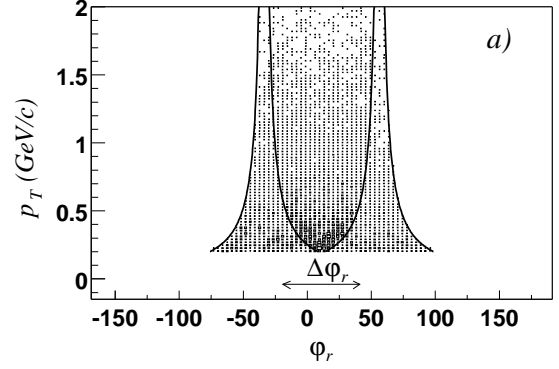


FIG. 3. a) The acceptance in reconstructed transverse momentum p_T and azimuthal angle φ_r . The solid curves indicate the acceptance bands for positive and negative particles, respectively. b) The effect on $v(Q)$ of varying the acceptance in φ_r . The solid curve shows the expectation from global charge conservation. The 10 % most central events are used for data and RQMD. (Angles in degrees.)